JOURNAL OF CATALYSIS 147, 186–198 (1994)

The Oxyiodination of Aromatic Compounds over Zeolite KX: The Case of Naphthalene

Gerald C. Tustin and Mark Rule

Eastman Chemical Company, Kingsport, Tennessee 37662

Received June 24, 1993; revised October 12, 1993

Aromatic compounds, iodine, and oxygen react in the vapor phase over basic faujasite zeolites at 225–350°C to produce iodoaromatic compounds and water. When the aromatic compound is naphthalene and the reaction is conducted in the region of 250°C over KX zeolite, a shape-selective catalytic oxyiodination occurs, resulting in predominant iodination at the 2-position of naphthalene. Typical product mixtures contain approximately 10% 1-iodonaphthalene, 65% 2-iodonaphthalene, 19% 2,6-diiodonaphthalene, 5% other diiodonaphthalene isomers, and 1% mixed triiodonaphthalene isomers at approximately 20% naphthalene conversion and 80–99% iodine conversion. Excessive conversion and excessive residence time reduce the selectivity to kinetic product, 2,6-diiodonaphthalene, but do not alter the selectivity for iodination in the 2-position. Selectivity for iodination in the 2-position is decreased by substituting sodium for potassium in the zeolite, by altering the faujasite zeolite Si/Al ratio significantly above or below 1.25, and by increasing the amount of iodine in the reactant feed. © 1994 Academic Press, Inc.

INTRODUCTION

Aromatic iodination reactions using molecular iodine as a reagent are among the most difficult halogenation reactions (1). The difficulty has been attributed to the low electrophilicity of iodine in its positive valence state and to poor equilibrium between the iodine and aromatic compound reactants and the hydrogen iodide and iodoaromatic compound products. Because of these difficulties most aromatic iodination reactions are performed under conditions promoting the formation of I^+ and also providing for the removal of the coproduct HI from the reaction (2). Occasionally a stoichiometric iodide trap, such as an Ag^+ ion (3), is used to drive the reaction. More often strong oxidizing agents, such as HNO_3/H_2SO_4, HIO_3/H_2SO_4, Ce(IV), and peracetic acid, have been used to accomplish these iodination reactions (2). One particularly interesting case reported by Radner uses $NOBF_4$, as a catalytic oxidant that is regenerated with molecular oxygen in a system containing iodine (or iodides) and the aromatic compound in a solvent system typically composed of trifluoroacetic acid and trifluoroacetic anhydride (4). The Radner method is thus an example of an oxyiodination whereby the unfavorable thermodynamics of the iodination are overcome by the formation of water which then reacts with trifluoroacetic anhydride. Typical electrophilic substitution patterns are observed with the Radner method, and a high para preference is observed when toluene is the substrate. Napthalene yields 1-iodonaphthalene (**1**) almost exclusively.

Recent reports in the patent literature reveal the use of zeolites as oxyiodination catalysts (5, 6). Paparatto and Saetti have described the zeolite-catalyzed oxyiodination of benzene (5). We have described a zeolite-catalyzed process for the shape-selective oxyiodination of several aromatic compounds (6), with particular emphasis placed on naphthalene and benzene (6b, c). The preferred catalyst for these reactions is zeolite X having the bulk of sodium ions exchanged with potassium ions (KX zeolite). The oxyiodination reactions are performed in the vapor phase by passing air, iodine (or, in some cases, vaporized aqueous HI or HI + iodine), and the aromatic compound over the catalyst at temperatures typically ranging from 225 to 350°C. The zeolite catalyzes the reaction without the addition of an oxidizing metal. The condensed product from these reactions is essentially free of tars and other by-products and consists entirely of iodoaromatic compounds, water, and unreacted starting materials. In many instances transiodination (disproportionation) reactions occur under conditions very similar to the oxyiodination reaction used to prepare the iodoaromatic compounds originally. Thus it is possible to prepare iodobenzene from a mixture of benzene and diiodobenzene by passing the reactants over NaX zeolite in a nitrogen stream in the presence of a small amount of iodine (used as a promoter) at 325°C (7).

A particularly interesting aspect of the zeolite-catalyzed oxyiodination reaction is the shape-selective nature of the

0021-9517/94 $6.00

substitution pattern; this is particularly striking in the case of naphthalene oxyiodination where 2-iodonaphthalene (**2**) is the predominant product. The most abundant diiodonaphthalene isomer produced in the KX zeolite-catalyzed oxyiodination reaction is 2,6-diiodonaphthalene (**3**), and it is even produced in greater abundance than 1-iodonaphthalene. Benzene yields diiodobenzenes containing 1,4-diiodobenzene as the predominant disubstituted isomer. However, the zeolite-induced shape selectivity effects observed in benzene oxyiodination are partly masked by the inherent ortho- , para-directing effects characteristic of halobenzenes, and, therefore, the shape selective effects observed with naphthalene are much more apparent.

This new oxyiodination chemistry offers new routes to commercially important products. For example, high molecular weight poly(phenylene sulfide) can be prepared by heating 1,4-diiodobenzene with sulfur in a salt-free, solvent-free system (8).

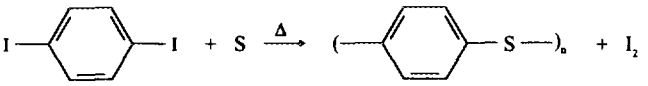

Recovered iodine can be reused in the oxyiodination reaction; 2,6-diiodonaphthalene can be carbonylated in methanol to the desirable polymer intermediate dimethyl 2,6-naphthalenedicarboxylate without the requirement of an added amine base (9).

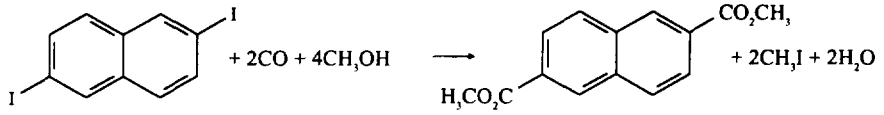

Iodine can be recovered from the methyl iodide for reuse in the oxyiodination reaction (10).

Here we describe studies designed to provide insight into the nature of the oxyiodination of naphthalene. The possible roles of disproportionation and isomerization are investigated. The effects of several aspects of catalyst structure, reaction conditions, and conversion on the rate and selectivity of the naphthalene oxyiodination reaction are examined. Possible mechanistic aspects of the reaction are discussed.

METHODS

Materials—general. Naphthalene (Texaco) was distilled. Iodine (Mallinckrodt, AR grade) was used without further purification. Pure 2-iodonaphthalene was isolated from oxyiodination product mixtures by fractional distillation followed by crystallization from methanol. Zeolites were obtained from Union Carbide Corporation (UOP) as powders and pellets of varying configuration and potassium exchange levels. Low-silica faujasite was prepared by the method of Kuhl (11). The 23-μm zeolite crystals were prepared by the method of Charnell (12). Potassium exchange into the low-silica faujasite and 23-μm crystals was accomplished by a modified version of the method of Hathaway and Davis (13) by stirring a zeolite slurry with 0.25 *M* aqueous KOH (50–70 ml per gram of zeolite) at room temperature overnight, decanting the exchange solution, repeating the exchange/decantation procedure until the desired exchange level was obtained (4 cycles for low silica faujasite, 5 cycles for the 23-mircron material), washing with water until the filtrate pH = 11, and air drying on the filter and then at 80°C overnight. All zeolites gave satisfactory X-ray diffraction patterns and elemental analyses. All zeolites were hydrated to constant weight by vapor equilibration over saturated aqueous ammonium sulfate solution before use in the naphthalene oxyiodination reaction or before X-ray diffraction studies. Relevant properties of the zeolites are provided in the tabulated data.

Analysis. Potassium, sodium, aluminum, and silicon contents of zeolite samples were determined by inductively coupled plasma optical emission spectroscopy and were recorded with a Perkin–Elmer Plasma 2000 instrument. Zeolite crystal particle size distributions were recorded with a MICROTRAC Model 9500 particle size analyzer. X-ray diffraction patterns were obtained by a Sintag PAD V diffractometer using a Cu$K\alpha$ source. Oxyiodination product mixtures were analyzed for napthalene and iodonaphthalenes through triiodonaphthalenes by a Hewlett–Packard Model 5890 gas chromatograph fitted with a 0.25-mm I.D. by 30-m long DB-17 liquid crystal capillary column programmed at 110°C for zero minutes, 6°C/minute to 250°C, and 250°C for 15 minutes with octadecane as an internal standard. Elemental iodine was determined by thiosulfate titration.

Naphthalene oxyiodination reactions—apparatus. Gas feeds for the reaction were provided by five Tylan Model FC-260 mass flow controllers having control ranges of 0–500 standard cubic centimeters per minute (SCCM). Naphthalene and iodine were fed by metering air through the molten materials held in separate glass vaporization vessels at 178 and 117°C, respectively. The naphthalene- and iodine-saturated air streams were conveyed to the glass reactor head via heat-traced glass transfer lines.The

reactor head contained ports for entry of the air/naphthalene and air/iodine streams and for additional air or nitrogen gas. A 9-mm O.D. quartz thermowell extended into the reactor, a 22-mm I.D. quartz tube 39 inches in length. The reactor tube was mounted vertically in a three-element electric Lindberg tube furnace having a heated chamber length of 24 inches. Products were collected in 500-ml vented bottles at ambient temperature. Temperature control and monitoring were provided by a Dow Model 2500 CAMILE system interfaced with an IBM PS/2 Model 55 SX computer.

Naphthalene oxyiodination procedure. This procedure provided the optimum performance detailed in Table 6. The reactor was loaded with sufficient coarse quartz chips to allow the catalyst to be positioned in the center of the furnace chamber. The hydrated KX zeolite (10.0 g, 14 ml, 16X40-mesh, 94% K-exchanged) was loaded on top of the quartz support zone, and additional coarse quartz chips were loaded on top of the catalyst to provide a mixing and preheat zone. A thermocouple was positioned in the center of the catalyst bed. The reactor was heated to 250°C with air (413 SCCM) flowing through the reactor, and then naphthalene (3.1 mmol/min) and its transpiration air (110 SCCM) were fed to the reactor. After the catalyst temperature returned from its maximum naphthalene adsorption exotherm (291°C) back to the 250°C set temperature, iodine (0.5 mmol/min) and its transpiration air (63 SCCM) were fed to the reactor. After 78 h of continuous reaction, the amount of air delivered to the reaction was increased to 989 SCCM. A sample (31.02 g) was collected between 102 and 103 h of continuous operation, and was melted on the steam bath and analyzed for organic components and for molecular iodine as described above. The air feed rate was reduced to 586 SCCM and nitrogen (400 SCCM) was fed to the reactor. A sample (31.98 g) was collected between 108 and 109 h of total continuous operation and analyzed as described above. Reaction was terminated by stopping the air/iodine feed to the reactor; then, after an additional 25 min, the air/naphthalene feed; finally, after an additional hour with only auxiliary air, the furnace was cooled and the reactor removed. Other naphthalene oxyiodination experiments were performed in a similar fashion.

Reaction-order and activation energy studies at low conversion. The apparatus described above was used to perform these studies. These studies were performed with 98% K-exchanged zeolite X pellets (1.00 g) ground to 60 × 200 mesh and diluted with 5-ml quartz fines. A fresh catalyst charge was used for each data point to minimize complications arising from catalyst deactivation. Samples were collected between the first and second hours of operation. Reaction-order studies were performed at a furnace setting of 250°C. The iodine reaction order study spanned iodine delivery rates ranging from a low of 0.25 mmol/min to a high of 2.00 mmol/min and was performed in increments of 0.25 mmol/min. Throughout the iodine reaction-order study, the naphthalene was maintained at 3.0 mmol/min, the oxygen was held at 5.39 mmol/min, and the total gas delivery rate was held at 739 SCCM by the addition of nitrogen to offset the volume changes resulting from changes in the amount of iodine fed. The naphthalene reaction-order study spanned naphthalene delivery rates ranging from a low of 1.0 mmol/min to a high of 6.0 mmol/min, and was performed in increments of 1.0 mmol/min. Iodine was maintained at 0.5 mmol/min throughout the naphthalene reaction-order study, oxygen was held at 5.39 mmol/min, and the total gas flow again was held at 739 SCCM. The oxygen reaction-order study ranged from 3.98 to 6.80 mmol O_2/min and was performed in increments averaging 0.5 mmol/min. Naphthalene and iodine were held at 3.0 and 1.25 mmol/min during the oxygen reaction-order study, and total gas delivery rate was 818 SCCM. The activation energy study was performed at feed rates of 1.0 mmol naphthalene/min, 0.5 mmol iodine/min, 5.39 mmol oxygen/min, and a total gas delivery rate of 739 SCCM. Catalyst bed temperatures ranged from 241 to 276°C (514 to 549°K) and were controlled by increasing the furnace temperature setting in 5° increments. A precision study was performed to determine the standard deviations in the weight percentages reported from gas chromatographic analysis of a typical sample produced under these low conversion conditions. The sample was analyzed 10 times and the following average weight percentage values and standard deviations were obtained: for **1**, 1.87 ± 0.063; for **2**, 6.23 ± 0.170; for **3**, 1.63 ± 0.020. The concentrations of the other iodinated naphthalenes were too low to provide meaningful rate data at low conversion.

Oxyiodination at high iodine and naphthalene conversions (Fig. 2). Three bed sizes of an 85% K-exchanged 8 × 16-mesh zeolite X catalyst were used in this study: 235, 470, and 940 cm^3. Nitrogen, air, naphthalene, and iodine were fed to the reactor at 8.0, 2.38, 1.0, and 0.5 mol/h, respectively, at a furnace set point of 280–290°C. Samples were taken at 20, 40, 60, and 80 h into each run, and the experiment with the 470-cm^3 bed was duplicated.

Oxyiodination at varying degrees of low iodine and naphthalene conversions (Fig. 3). Four bed sizes of a 92% K-exchanged 16 × 40-mesh zeolite X were used in this study: 1, 5, 10, and 20 g. Air (575 SCCM) was fed to the reactor along with iodine (0.5 mmol/min) and naphthalene (3.0 mmol/min) at a furnace set point of 250°C. Samples were taken at 2, 7, and (with the larger catalyst beds) 10 h into each run.

Sequential oxyiodination/disproportionation study (Fig. 4). Two sequential glass reactors were used in this

study. Continuous oxyiodination was performed in the first reactor and continuous disproportionation was performed in the second reactor. The oxyiodination reactor contained 92% K-exchanged 16 × 40-mesh zeolite X (119.78 g) held at 280°C; naphthalene (0.75 mmol/min), iodine (0.75 mmol/min), and air (148 SCCM) were fed to the reactor. The volatile materials from the oxyiodination reactor (primarily unused air and steam) were vented from a heated collection manifold held at 100–120°C. The molten material collected in a U-tube fitted with a sampling stopcock. The overflow material from the U-tube flowed into the inlet manifold of the disproportionation reactor where additional naphthalene (2.25 mmol/min), nitrogen (86 SCCM, used to transpire the naphthalene to the manifold), and air (25 SCCM) were also added. The pressure differential across the U-tube compensated for the pressure drop across the disproportionation reactor which contained the same catalyst (293.18 g) used in the oxyiodination reactor held at 250°C.

RESULTS AND DISCUSSION

General characteristics of the KX zeolite-catalyzed oxyiodination of naphthalene. A typical oxyiodination reaction over a KX catalyst exhibits a remarkable selectivity to iodination in the 2-position, and, of the products produced, over 80 mol% consists of **2** and **3** with the balance being **1,** all other isomers of diiodonaphthalene (O-DIN) and 1% or less of mixed isomers of triiodonaphthalene (TIN):

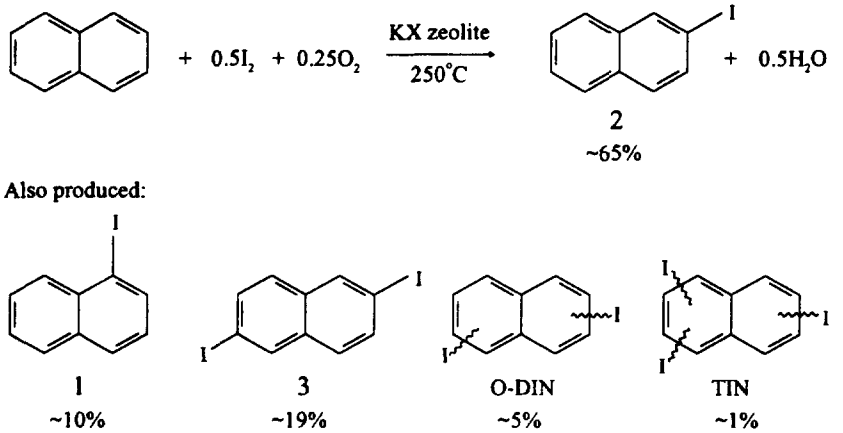

An approximate indicator of the selectivity to iodination in the 2-position is the 2-to-1 substitution ratio, defined as the ratio of the sum of the mole percentages of **2, 3,** and 2,7-diiodonaphthalene (**4**) to **1.** Values of the 2-to-1 substitution ratio exceeding 10 have been observed under optimum operating conditions. Although many parameters alter the selectivity to **3,** only three affect the value of the 2-to-1 substitution ratio significantly: the exchange of potassium for sodium in the zeolite, the Si/Al ratio in the zeolite, and the amount of iodine fed.

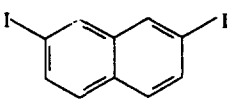

4

The effect of potassium exchange. The effects of replacing the sodium ions native to zeolite X with potassium are shown in Table 1. Although the activity with the NaX catalyst is somewhat greater than that of the KX material, the 2-to-1 substitution ratio resulting from use of NaX is less than one third that resulting from use of KX. A much higher selectivity to diiodonaphthalenes and triiodonaphthalenes is also apparent with the KX material. Also, the selectivity to the 2,6-isomer **3** within the diiodonaphthalenes and triiodonaphthalenes is significantly higher with the KX catalyst. A more subtle effect resulting from the presence of potassium in the zeolite is described in the section on activation energy.

The effect of silicon-to-aluminum ratio. The ratio of silicon to aluminum in the faujasite structure can vary considerably, proceeding from a low of 1.0 in low silica faujasite through about 1.25, common for zeolite X, to above 2.4 and higher for zeolite Y (14). The results of progression through this series on the napthalene oxyiodination reaction are striking, and these are summarized in Table 2. The preference for 2-iodination is very apparent for the X-type catalysts as reflected by the 2-to-1 substitution ratios. The highest selectivity to **3** was observed at Si/Al = 1.25. Low activities and conversions were observed at the low and the high extremes of Si/Al ratios. Comparison among the catalysts operating at different

TABLE 1

Effects of Potassium Exchange

	NaX	KX (98% exchanged)
sty[a] **1**	2.41	0.76
sty **2**	6.94	5.74
sty **3**	0.21	1.49
sty O-DIN	0.42	0.48
sty TIN	0	0.03
mol% **1**	24.2	8.9
mol% **2**	69.5	67.5
mol% **3**	2.1	17.5
mol% O-DIN	4.2	5.7
mol% TIN	0	0.4
Naphthalene conversion (%)	23.5	19.7
Iodine conversion (%)	91.6	91.2
2-to-1 substitution ratio[b]	3.0	9.8
3/(O-DIN + TIN) ratio	0.5	2.9
Hours on stream	2	2
Bed temperature (°C)	262	269

[a] Space time yield, mol/(kg-h).

[b] (mol% **2** + mol% **3** + mol% **4**)/(mol% **1**). Conditions: 4.2 g (16 × 40 mesh) zeolite X, furnace temperature = 250°C, 3.1 mmol naphthalene/min, 0.5 mmol iodine/min, 575 standard cubic centimeters per minute (SCCM) air.

conversion levels is difficult, but it becomes more apparent from the section on conversion effects that operation at higher conversions at the two extremes of the Si/Al ratio would not make these catalysts perform more like those in the middle range. The KY zeolite was different from all of the others in that it produced monoiodonaphthalenes and very little polyiodinated naphthalenes.

Diffusion effects. Diffusion effects are relevant to most heterogeneous catalyzed reactions, especially those involving zeolite catalysts (15). In the present system both intrapellet and intrazeolite diffusion effects are very important. The intrapellet effects are described first. Most of the results described (except when noted otherwise) were obtained by using material ground to 16 × 40 mesh. Smaller sizes were used when powders were evaluated or when more detailed activation energy or reaction-order studies were being performed. The intrapellet effectiveness factor for the reaction was determined in a preliminary study on the effect of particle size on the activation energy; the effectiveness factor approached 1.0 only when the particle size was on the order of 0.1 mm. Owing to the experimental difficulties involved with particles this small, they were only used when essential for mechanistic information (reaction order and activation energy study). The effects of using 8 × 14-mesh and 16 × 40-mesh catalysts are shown in Table 3. The main effects of reduction of pellet size on the reaction are increases in the production rates of **1** and **2** and in the iodine and naphthalene conversions. One effect resulting from the reduction in pellet size is large increase in the production rate of **1** which is compensated for by a decrease in the O-DIN production rate. This phenomenon is partially responsible for the small shift in the 2-to-1 substitution ratio. Although a reduction in pellet size decreases the total amount of di- and triiodonaphthalenes produced, the ratio **3**/(O-DIN + TIN) actually increases slightly as a result of this change. We have investigated several different forms of catalyst particles, and differences in intrapellet diffusion effects among different catalysts are common. In some cases outer shell barriers provided significant diffusion resistance to the reactions. Grinding catalysts to 16 × 40 mesh reduced the differences in diffusion properties among various batches of catalyst to allow for more direct comparisons.

An investigation into the nature of intrazeolite diffusion effects was also performed. In this study the

TABLE 2

Effects of Catalyst Si/Al Ratio

Si/Al =	1.0	1.25	1.35	1.45	2.4
sty **1**	1.47	0.94	0.96	1.17	1.80
sty **2**	3.25	6.48	7.12	7.39	1.85
sty **3**	0.69	1.33	1.11	1.03	0.06
sty O-DIN	0.26	0.52	0.50	0.53	0.11
sty TIN	0.05	0.01	0.02	0.02	0
mol% **1**	25.7	10.2	9.9	11.6	47.1
mol% **2**	56.8	69.8	73.3	72.8	48.5
mol% **3**	12.1	14.4	11.4	10.2	1.6
mol% O-DIN	4.6	5.6	5.2	5.2	2.8
mol% TIN	0.8	0.1	0.2	0.2	0
Naphthalene conversion (%)	9.3	21.8	22.9	23.3	10.0
Iodine conversion (%)	44.1	96.1	97.4	96.0	39.5
2-to-1 substitution ratio	2.7	8.5	8.8	7.3	1.1
3/(O-DIN + TIN) ratio	2.2	2.5	2.1	1.9	0.6
Hours on stream	2	2	2	2	2
Conditions[a]	A	B	B	B	B

[a] Conditions: A = 3.32 g loosely aggregated binderless KX zeolite powder (96% K-exchanged), furnace temperature = 250°C, 3.1 mmol naphthalene/min, 0.5 mmol iodine/min, 575 SCCM air; B = 4.2 g 16 × 40-mesh KX zeolite particles containing 20 wt% binder (98% K-exchanged), furnace temperature = 250°C, 3.1 mmol naphthalene/min, 0.5 mmol iodine/min, 575 SCCM air.

TABLE 3

Effects of Catalyst Mesh and Crystal Sizes[a]

	8 × 14 mesh	16 × 40 mesh	2.2 μm	23 μm
sty **1**	0.61	0.83	0.83	0.46
sty **2**	4.56	5.25	5.00	2.70
sty **3**	1.32	1.32	1.27	0.78
sty O-DIN	0.34	0.29	0.28	0.29
sty TIN	0.02	0	0.04	0.04
mol% **1**	8.9	10.9	11.2	10.9
mol% **2**	66.5	68.3	67.5	62.9
mol% **3**	19.3	17.2	17.1	18.2
mol% O-DIN	5.0	4.3	3.8	6.9
mol% TIN	0.4	0	0.5	0.9
η_1 (effectiveness factor)	0.86	0.90	1.0	0.50
η_2	0.85	0.95	1.0	0.50
η_3	1.0	1.0	1.0	0.62
$\eta_{O\text{-}DIN}$	0.95	0.85	1.0	1.0
η_{TIN}	—	—	1.0	1.0
Naphthalene conversion (%)	15.5	18.4	12.3	8.7
Iodine conversion (%)	75.7	86.1	57.1	52.7
2-to-1 substitution ratio	9.9	7.8	7.7	7.7
3/(O-DIN + TIN) ratio	3.6	4.0	4.0	2.4
Hours on stream	2	2	2	2
Conditions[b]	A	A	B	C

[a] Effectiveness factors estimated by the triangle method (16).

[b] Conditions: all experiments were performed at furnace temperature = 250°C, 3.1 mmol naphthalene/min, 0.5 mmol iodine/min, 575 SSCM air; A = 4.2 g KX zeolite (96% K-exchanged, 20% binder); B = 3.32 g binderless KX powder (99.3% K-exchanged, Si/Al = 1.26); C = 3.32 g binderless KX powder (98.4% K-exchanged, Si/Al = 1.36).

performance of large zeolite crystals having an average particle size of 23 μm was compared to that of 2.2-μm crystals at a similar exchange level under the same reaction conditions. The effects of this change are also summarized in Table 3. All space time yields decreased when the crystal size was increased except those of O-DIN and TIN which remained essentially unchanged. A small increase in the mole percentage of **3** was accompanied by a much larger relative increase in the O-DIN and TIN. The mole percentages of both **2** and **1** decreased. The value of the 2-to-1 substitution ratio was not affected by this large change in crystal size. A more subtle diffusion effect resulting from changing the amount of potassium in the zeolite is described in the following section on activation energy.

Activation energy study. The activation energy study was performed at low conversion and under conditions designed to minimize intrapellet diffusion effects. Figure 1 is the Arrhenius plot for the rate data obtained with the 98% K-exchanged zeolite X, and the calculated activation energies are provided in Table 4. The plot in Fig. 1 shows an obvious onset of curvature with increasing temperature, and this is particularly obvious in the cases of **1** and **2**. Higher temperatures appear attainable in the case of **3** before the onset of curvature. Curvature in the Arrhenius plot generally indicates the transfer from a kinetic to a diffusion regime (17). Extreme curvature (to the point of indicating negative activation energies) is quite common in zeolite catalysis and can result when the heats of adsorption of reactants are high and a strong intracrystalline diffusion limitation exists as well (15). Accelerated catalyst deactivation at elevated temperature can also produce curvature, and this cannot be discounted as a possibility in the case of the 98% K-exchanged zeolite X. However, no apparent curvature was observed in the Arrhenius plots from an 89% K-exchanged zeolite X activation energy study. The values for the activation energies found with the 89% K-exchanged zeolite X were essentially the same

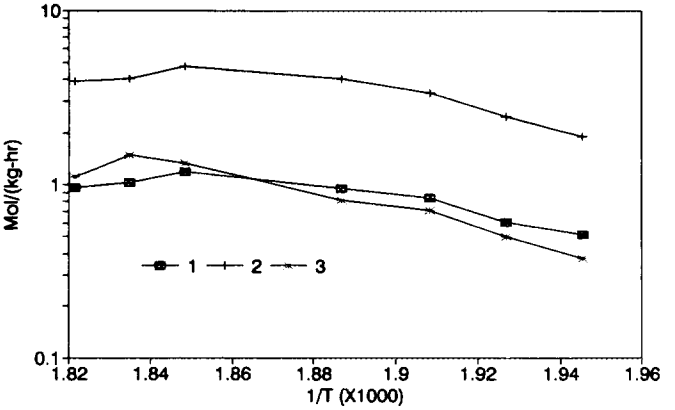

FIG. 1. Arrhenius plot fo the space time yields of **1**, **2**, and **3** observed with a 98% K-exchanged zeolite X catalyst.

TABLE 4

Activation Energies and Reaction Orders for the Formation of 1, 2, and 3

Property	**1**	**2**	**3**
Ea (kcal/mol)	22.0 ± 3.1[a]	25.9 ± 2.4[a]	24.2 ± 1.4[b]
Reaction orders in			
Iodine	0.33 ± 0.12	−0.24 ± 0.12	−0.14 ± 0.16
Naphthalene	0.35 ± 0.18	0.53 ± 0.09	0.19 ± 0.21
Oxygen	0.80 ± 0.25	0.96 ± 0.18	1.51 ± 0.17

[a] Calculated from the first four low-temperature points.

[b] Calculated from the first six low-temperature points.

TABLE 5

Effects of Iodine Level at Higher Conversions

	I_2 feed rate (mmol/min)		
	0.5	1.0	2.0
sty **1**	0.37	0.55	0.59
sty **2**	2.6	2.4	1.8
sty **3**	0.36	0.95	0.91
sty O-DIN	0.18	0.26	0.29
sty TIN	0.01	0.03	0.04
mol% **1**	10.8	13.2	16.1
mol% **2**	65.8	57.3	50.0
mol% **3**	18.3	22.7	24.9
mol% O-DIN	5.0	6.1	8.0
mol% TIN	0.17	0.62	1.1
Naphthalene conversion (%)	21.4	27.9	24.6
Iodine conversion (%)	94.8	67.5	34.1
2-to-1 substitution ratio	7.9	6.2	4.8
3/(O-DIN + TIN) ratio	3.5	3.4	2.7
Hours on stream	2	4	6
Conditions[a]	A	B	C

[a] Conditions: 13.28 g loosely aggregated binderless KX zeolite powder (99.2% K exchanged), furnace temperature = 250°C, 3.1 mmol naphthalene/min; A = 573 SCCM air; B = 639 SCCM air; C = 762 SCCM air.

as those found for the 98% K-exchanged zeolite X. Thus it appears that increasing the potassium level from 89 to 98% lowers the temperature where the transfer to a diffusion-controlled regime occurs.

Reaction-order studies and feed ratio effects. The reaction-order study was performed under conditions designed to keep the naphthalene and iodine conversions in the region of 5 to 10% to best approach differential operating conditions. The results of the reaction-order study are also summarized in Table 4. The precision of this study is less than desired because of the variable amounts of product that transported through the receiver when the reaction was performed at such high gas velocities and low conversions. Nevertheless, the reaction orders do reveal several important features of the kinetic behavior of the naphthalene oxyiodination reaction. For example, even when the variance of the measurements is considered, the reaction orders in iodine for the production of **1** (slightly positive) are different than those for the production of **2** and **3** (both slightly negative). Another salient feature of the reaction-order study is the difference observed in the oxygen reaction orders between the production rates of **1** and **2** (both approximately first order) and **3** (approximately 1.5 order).

The iodine reaction-order effects seen at low conversion are also apparent at the higher conversions found under more typical operating conditions. The results are summarized in Table 5. Although the amount of air present was also increased somewhat along with the iodine, the primary effects seen are due to the increased levels of iodine. The significant decrease in the 2-to-1 substitution ratio is another indication of the negative iodine reaction order for 2-substitution and the positive iodine reaction order for 1-substitution. The inhibitory effect of iodine beyond a certain level is also reflected in the failure to increase the naphthalene conversion when the iodine feed rate is increased from 1.0 to 2.0 mmol/min.

The effects of changing the amount of oxygen present at higher conversions are summarized in Table 6. When the amount of oxygen present was decreased, essentially no change in the space time yield of **2** was observed, but the space time yield of **3** decreased significantly. Thus the oxygen reaction-order effect seen at low conversion for the production of **2** is not apparent at higher conversion, although it is at least partially apparent for the production of **3**.

Conversion effects. The relationships among bed size, conversion, and selectivity were investigated in a two-part study. Three different bed sizes of an 85% K-exchanged zeolite KX catalyst were used in the first part of the study at various degrees of catalyst deactivation.

TABLE 6

Effects of Replacing a Portion of the Air with N_2

	989 SCCM air	586 SCCM air + 400 SCCM N_2
sty **1**	0.28	0.32
sty **2**	2.06	2.09
sty **3**	0.83	0.63
sty O-DIN	0.18	0.19
sty TIN	0.03	0.02
mol% **1**	8.3	9.8
mol% **2**	60.7	64.5
mol% **3**	24.7	19.4
mol% O-DIN	5.4	5.7
mol% TIN	0.8	0.6
naphthalene conversion (%)	17.7	17.0
iodine conversion (%)	82.7	72.4
2-to-1 substitution ratio	10.6	8.8
3/(O-DIN + TIN) ratio	4.0	3.1
Hours on stream	103	109
Bed temperature (°C)	256	258

Note. Conditions: 10.0 g (14 mL) 16 × 40-mesh KX zeolite (96% K exchanged), furnace temperature = 250°C, 3.1 mmol naphthalene/min, 0.5 mmol iodine/min.

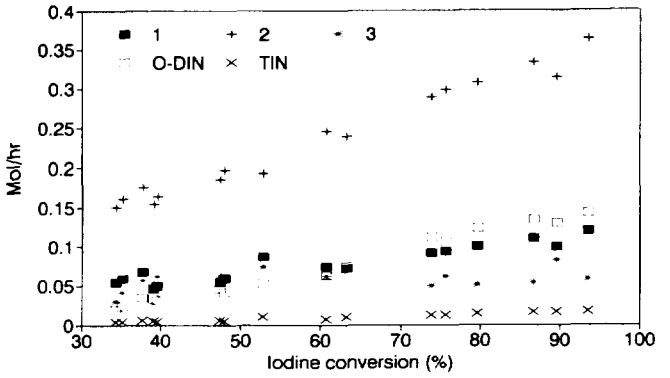

FIG. 2. Hourly yields of **1**, **2**, **3**, O-DIN, and TIN observed at 27–62% naphthalene conversion as a function of iodine conversion.

Conditions were selected to allow for especially high naphthalene conversions (27–62%). Figure 2 is a plot of the moles of product produced per hour (independent of the amount of catalyst present) as a function of iodine conversion observed in this reaction. The extent of reaction is sufficiently high in this case to cause the production rate of **3** to be at a steady state throughout the entire conversion range studied. The other products continue to increase as the conversion increases. The second part of the conversion study examined the reaction at a lower extent of reaction. Figure 3 is a plot of the mmoles of product produced per hour as a function of iodine conversion, but at only 2 to 27% naphthalene conversion. Figure 3 indicates that the amount of **3** continues to increase in the early part of the reaction and then reaches a steady state as the iodine conversion is increased further. The relative amounts of the other components continue to increase as the conversion increases. Thus the results from the conversion (or extent of reaction) experiments suggest that **3** is indeed a kinetic product, and that it is subsequently converted to other products upon extended reaction.

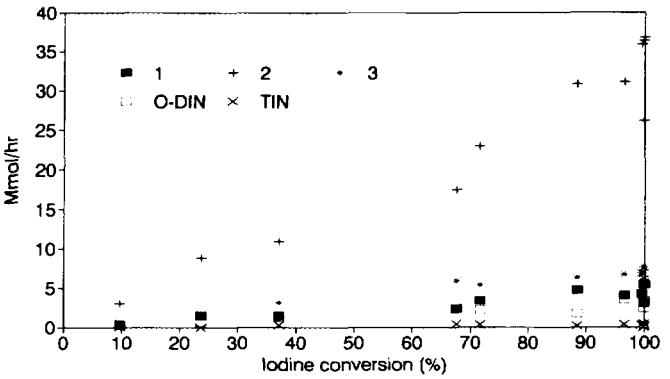

FIG. 3. Hourly yields of **1**, **2**, **3**, O-DIN, and TIN observed at 2–27% naphthalene conversion as a function of iodine conversion.

The possible roles of disproportionation and isomerization reactions occurring during oxyiodination. The preceding description of conversion effects and the notion that the kinetic product **3** is converted to other products raise the possibility that other reactions along with continued oxyiodination may be partially responsible for the shift in selectivity. In view of the known fact that isomerization and disproportionation reactions occur with similar catalysts under similar reaction conditions (7), additional experiments were performed to determine whether these same reactions were occurring to a significant degree with the KX catalyst under optimum operating conditions. The first of these experiments was the oxyiodination of pure 2-iodonaphthalene. The pure **2** feed material contained no detectable naphthalene or **1**. The results of this experiment are summarized in Table 7. Although oxyiodination occurred to produce mainly **3**, the conversion of **2** into **1** and naphthalene is negligible under these conditions.

The possible role of hydrogen iodide was also examined. The stoichiometric reaction between **2** and hydrogen iodide was examined both with and without the KX catalyst. The results of these experiments are also summarized in Table 7. Molecular iodine was produced in both reactions. Thus the iodination reaction is reversed by the action of a stoichiometric amount of HI. This same reaction also occurs when the catalyst is omitted, but the rate is much slower. Both of these experiments confirm the notion that the action of a

TABLE 7

Reactions of Pure 2-Iodonaphthalene

		Stoichiometric HI		
	Oxyiodination	With KX	Without KX	Pulsed HI
mol% naphthalene	0.8	91.5	16.6	9.3
mol% **1**	0.1	0	0	0.3
mol% **2**	83.6	8.2	83.6	88.4
mol% **3**	12.9	0.2	0	1.6
mol% O-DIN	2.5	<0.1	0	0.5
mol% TIN	<0.1	0	0	0
Conditions[a]	A	B	C	D

[a] Conditions: A = 3.11 g 8 × 14-mesh KX zeolite, furnace temperature = 250°C, 1.55 mmol **2**/min, 0.35 mmol iodine/min, 885 SCCM air, 400 SCCM nitrogen, 50 SCCM He; B = 3 mg 20 × 40-mesh KX zeolite, 22 mg **2** in a 150-ml tube evacuated and backfilled with 200 torr anhydrous HI, heated at 250°C for 1 h; C, same as B but with zeolite omitted; D = 1.0 g 16 × 40-mesh KX zeolite, ca. 100 ml HI pulsed into a nitrogen stream passing through a melt of 10 g **2** held at 250°C.

stoichiometric amount of HI can reverse the iodination reaction under conditions similar to those occurring during normal oxyiodination. The evidence for disproportionation becomes more apparent when less than a stoichiometric amount of HI is used. This experiment indicates that, in the presence of the KX catalyst, the action of less than a stoichiometric amount of HI results in disproportionation as well as in the reversal of the iodination reaction. None of the experiments with anhydrous HI produced significant amounts of **1**.

Another experiment was performed to investigate the isomerization and transiodination possibility further. The feed material for this run was the product from a previous reaction from which all of the naphthalene and a portion of the monoiodonaphthalenes had been removed. The results from the prolonged heating of this material in air with a small amount of iodine in the presence of the KX catalyst are summarized in Table 8. The small changes in the product mix appear to be more indicative of further oxyiodination from the 2% iodine present rather than any significant degree of isomerization.

The preceding disproportionation/isomerization experiments were performed under conditions where naphthalene was absent from the reaction mixture, and the following experiment revealed the importance of the presence of naphthalene in the disproportionation reactions that occur during the oxyiodination process. This experiment featured an oxyiodination reactor connected in series to a disproportionation reactor. Naphthalene was added to the oxyiodination reactor product, and the mixed stream was fed to a second reactor containing the same KX catalyst. The two reactors were operated in this fashion for a period in excess of 200 h; the product mole percentages from each reactor are shown in Fig. 4. Sample numbers 2, 5, 9, 13, and 18 were taken from the oxyiodination reactor. All other samples were taken from the disproportionation reactor. The data depicted in Fig. 4 definitely show that disproportionation does occur with the KX catalyst when naphthalene is present. The low amount of **3** relative to the amounts of O-DIN and TIN in these

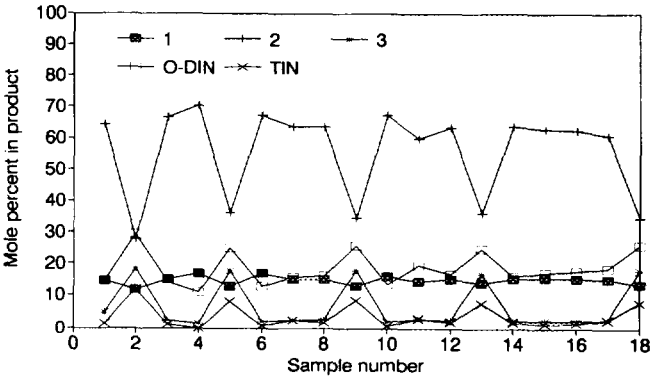

FIG. 4. Product mole percentages of **1**, **2**, **3**, O-DIN, and TIN produced in the oxyiodination reactor (samples 2, 5, 9, 13, and 18) and those produced from the downstream disproportionation reactor (all remaining samples); sample numbering is chronological.

experiments is due to the high iodine levels and high conversions in the first reactor. There is no evidence that any significant degree of isomerization occurred in the second reactor, and the 2-to-1 substitution ratio in the product from the disproportionation reactor (4.4–4.9) was essentially the same as that from the oxyiodination reactor (4.95–5.1). Related experiments with KX catalyst also showed that disproportionation occurs in the presence of naphthalene without significant isomerization whether air is present or not.

Isomerization accompanying disproportionation was observed only when strong acid catalysts were used. Table 9 summarizes the results observed with the strong acid catalyst SK-500 (a rare earth-exchanged Y zeolite) when naphthalene is added to mixed iodonaphthalenes in the liquid phase. This mixture is likely the equilibrium mixture since essentially the same mixture was obtained with different strong acid catalysts, with longer reaction times and with larger amounts of catalysts. KX and NaX catalysts were not active under these liquid-phase batch conditions.

In summary, disproportionation can occur under condi-

TABLE 8

Attempted Isomerization/Disproportionation of Naphthalene-Free Iodonaphthalenes with KX Catalyst

	Starting mixture	Product mixture
mol% naphthalene	0	0
mol% **1**	5.9	6.2
mol% **2**	16.6	13.4
mol% **3**	60.7	62.4
mol% O-DIN	12.8	14.0
mol% TIN	4.0	4.1

Note. Conditions: 0.42 g 16 × 40-mesh KX zeolite, 20.0 g mixed iodonaphthalenes, 0.4 g iodine, 57 SCCM air passed through mixture for 4 h at 250°C.

TABLE 9

Isomerization/Disproportionation of Iodonaphthalenes with SK-500 Catalyst[a]

	Starting mixture[b]	Product mixture[b]
mol% **1**	7.8	30.3
mol% **2**	20.8	53.1
mol% **3**	19.5	1.7
mol% O-DIN	32.5	7.1
mol% TIN	19.2	7.7
2-to-1 substitution ratio	6.8	1.9

[a] Conditions: 1.0 g SK-500 zeolite, 2.5 g starting mixture, 2.5 g naphthalene, heated 1 h at 250°C.

[b] Composition on a naphthalene-free basis.

tions similar to those used in oxyiodination with the KX zeolite catalyst present. Disproportionation is especially apparent under oxyiodination conditions when naphthalene is present, but is not apparent when naphthalene is absent. Although isomerization is observed with strong acid catalysts, there is no evidence that significant isomerization occurs during oxyiodination when the catalyst is KX zeolite. An example of one of the possible disproportionation reactions occurring among naphthalene, **2**, and **3** is illustrated in Scheme 1.

Mechanistic aspects of the oxyiodination reaction. Although no published work directed toward the zeolite-catalyzed oxyiodination reaction exists outside of the patent literature, the sequence depicted in Scheme 2 is consistent with our observations and those of literature reports on certain related aspects of the chemistry. Scheme 2 illustrates possible steps occurring when naphthalene is converted into 2-iodonaphthalene (**2**) and water

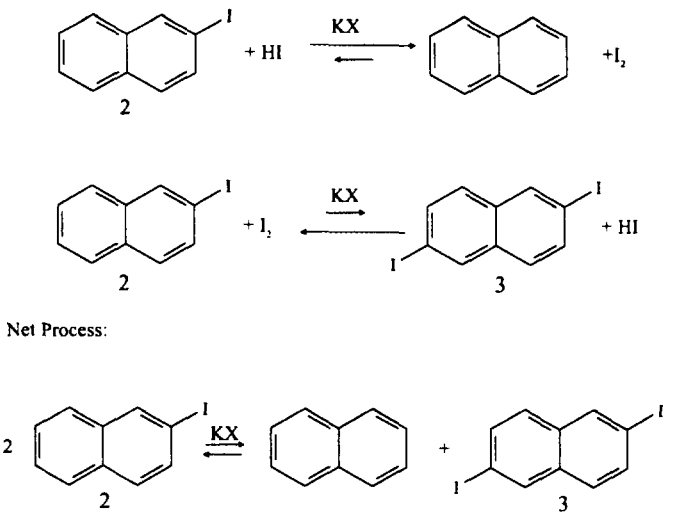

SCHEME 1

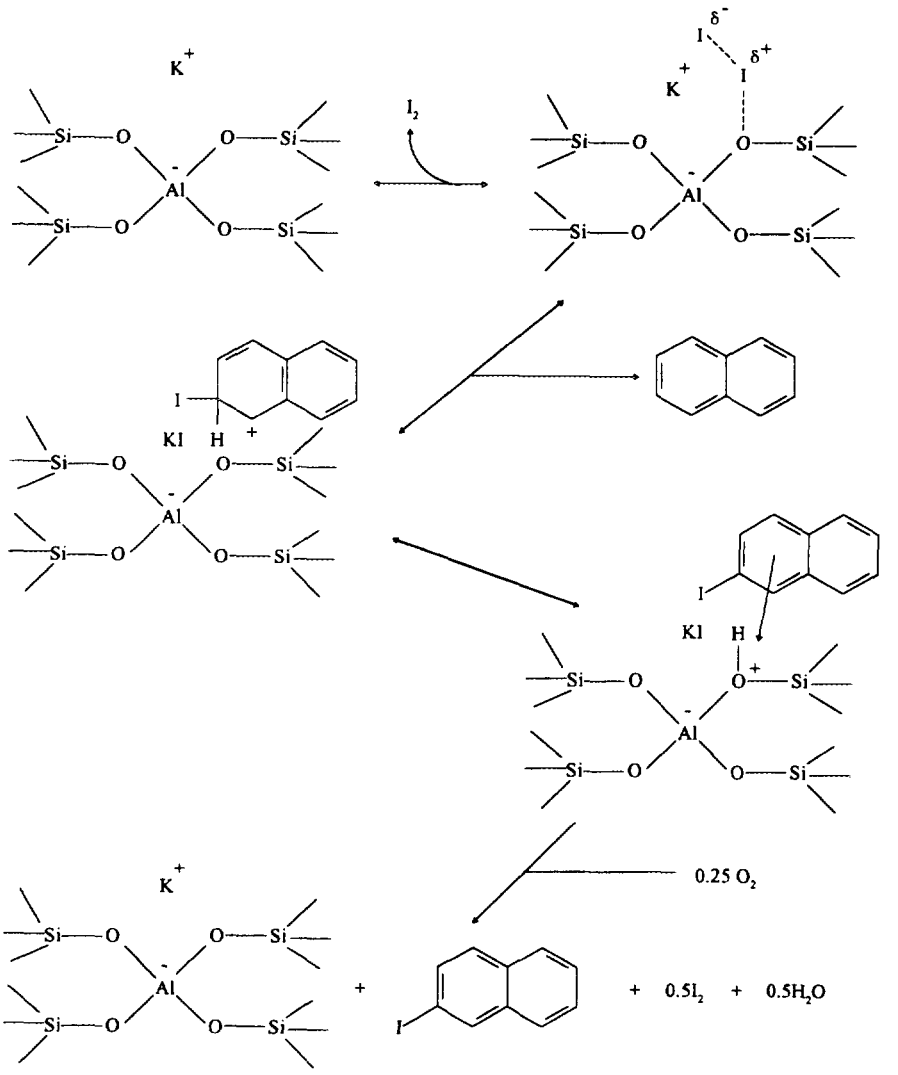

SCHEME 2

by reaction with molecular iodine and molecular oxygen in the presence of a KX zeolite. The first step depicted in Scheme 2 is the reversible adsorption of iodine at the aluminate site in the zeolite. The interaction of iodine with zeolite X is very strong. Adsorption studies reported by Barrer and Wasilewski indicated that initial heats of adsorption of iodine on zeolite X are above 25 kcal/mol, and, at saturation at 265°C, the zeolite contains about 1 g of iodine per gram of outgassed zeolite (18). At 20–40 mm Hg iodine pressure at 265°C, the outgassed zeolite adsorbs 400–500 mg iodine per gram. Barrer and Wasilewski observed a heterogeneity in the adsorption energy with coverage, and proposed that the zeolite's high initial affinity for iodine was due to the interaction of the polarizable iodine molecule with the alkali metal–aluminate exchange sites in the zeolite where strong coulombic fields and field gradients exist.This same type of interaction has been used to describe the high affinity of aluminum-rich zeolites for a number of polar molecules including water (19). Barrer and Wasilewski calculated that upon continued iodine pressure increases, the adsorption occurred on the exposed oxygens that comprise the wall of the zeolite cavity.

Our results are consistent with those of Barrer and Wasilewski, and this is reflected in the very low (or even negative) reaction orders observed with iodine. Common kinetic treatments, such as the Langmuir–Hinshelwood method, often attribute very low or negative reaction orders to a reactant that is very strongly adsorbed (20). Transport effects can also alter reaction orders (21), and should be considered when using Langmuir–Hinshelwood treatments (15, 22), especially with zeolites. Current data do not allow the determination of the relative contributions of adsorption and transport effects to the observed iodine reaction orders. However the kinetic data, coupled with the iodine adsorption data of Barrer and Wasilewski and other published work on aromatic iodination reactions (23, 24), lead us to speculate that iodine is adsorbed at the aluminate site to a sufficiently high degree to polarize it to I^+ and I^-, and that the I^+ is a sufficiently strong electrophile to attack aromatic molecules to form a sigma complex by the reversible reaction with adsorbed naphthalene. Kabalka, Pagni, and co-workers have described similar interactions in the stoichiometric reaction of iodine with aromatic molecules over dehydrated alumina (23). While other mechanisms, such as single electron transfer, are possible, the work of Galli suggests that a sigma complex mechanism for the iodination reaction is operative in all known cases (24). The naphthalene adsorption sites associated with this reaction are not depicted in Scheme 2. Although it is known that naphthalene and other aromatic hydrocarbons also show an initial adsorption affinity for the cation sites in faujasite zeolites (25, 26) it is also possible that naphthalene adsorbed on the wall near the cation site is the species that is actually attacked by the I^+ species existing at the cation site.

Since zeolite X (and KX in particular) is a basic zeolite (27), loss of a proton from the sigma complex produces product adsorbed at the conjugate acid site in the zeolite as depicted in Scheme 2. Ozin *et al.* have described similar conjugate acid species produced by the action of HCl, HBr, and HI on zeolite NaY (28). The reaction sequence to this point is entirely reversible, and this was confirmed by the observation that HI and **2** react over the zeolite to form naphthalene and molecular iodine.

The driving force for the reaction sequence is the oxidation reaction. The mechanism of the oxidation part of the reaction sequence has not been studied in our system. Uncatalyzed gas phase oxidation of hydrogen iodide occurs under similar conditions of temperature and pressure via a radical pathway (29). The possibility that the sigma complexes are oxidized instead of the deprotonated products complexed to the conjugate acid site cannot be excluded at this time. The observation of a higher oxygen reaction order for the formation of the diiodonaphthalene **3** than for **2** is consistent with sequential oxidations being required for each additional iodine placed on the naphthalene ring (30), although other effects could account for the oxygen reaction orders observed in a reaction system this complex.

The reverse iodination reaction, which was alluded to in Schemes 1 and 2, must be considered in understanding the 2-to-1 substitution ratios observed. It is interesting that conditions that increase the residence time of **2** and **1** in the zeolite (e.g., higher conversions resulting from larger catalyst beds, larger zeolite crystals, etc.) do not appear to interconvert **2** and **1** as measured by the 2-to-1 substitution ratio. In fact two of the three parameters that do alter the 2-to-1 substitution ratio change the structural and electronic character of the active sites (the degree of potassium exchange and the silicon-to-aluminum ratio). We speculate that the rates of initial iodination of naphthalene to produce zeolitic **1**.HI.KOZeol and **2**.HI.KOZeol, and the rates of the reverse reactions could be fast enough to establish a pre-equilibrium. The experimentally confirmed reversibility of the iodination reaction suggests that such a pre-equilibrium is possible. Furthermore, the position of this equilibrium likely favors starting materials over the products as illustrated by the observation that **2** retroconverts to naphthalene and iodine but not to **1** in the presence of HI and the absence of oxygen. A pre-equilibrium requires that the rate of oxidation be slow compared to that of equilibration, and no firm evidence exists to confirm this notion. Although the high reaction order in oxygen is consistent with the possibility that oxidation is slow compared to iodination, other effects could cause the oxygen dependency observed in this complex reaction system. However, if the rates of

oxidation of **1**.HI.KOZeol and **2**.HI.KOZeol are slow compared to the rate of equilibration among **1**.HI.KOZeol, **2**.HI.KOZeol, KX zeolitic naphthalene, and KX zeolitic iodine, then the pre-equilibrium could determine the relative amounts of the iodination occurring in the 2-position and in the 1-position. This pre-equilibrium could be such that iodination in the 2-position is favored over iodination in the 1-position by about 7–10 to 1 in KX zeolite. This phenomenon could be responsible for the shape-selective effects observed in this reaction. Oxidation irreversibly drives the reaction to completion. A change in the structure of the active site thus would change the actual reaction that is in pre-equilibration. The actual structural features of the active sites responsible for iodination at the 2-position are unknown at this time. The high selectivity to the diiodonaphthalene **3** could be due to catalyst shape selectivity effects, to a resonance effect resulting from the first iodine at the 2-position, or to a combination of both effects.

Some of the selectivity effects seen in the naphthalene oxyiodination reaction are also due to the expected relative ease of sequential iodination. Since iodine is ring deactivating, it should become progressively more difficult to add additional iodine to the ring system (31). However, although conventional iodination yields mainly monoiodinated aromatic products, the KX zeolite catalyzed oxyiodination reaction produces considerable diiodinated product. The KX catalyst appears to have sufficient iodination reactivity to place the second iodine into the naphthalene ring, but apparently the presence of the second iodine on the ring system deactivates the molecule sufficiently to keep the TIN production low. Diffusion effects appear to influence the degree of polysubstitution significantly. Disproportionation reactions arising from diffusion or conversion effects also affect the relative amounts of mono- , di- , and triiodonaphthalenes produced.

CONCLUSIONS

The oxyiodination of naphthalene over a faujasite zeolite catalyst produces a ratio of 2-iodonaphthalene to 1-iodonaphthalene that depends largely on the degree of potassium exchange, the silicon-to-aluminum ratio, and the amount of iodine used. Appreciable isomerization between 2-iodonaphthalene and 1-iodonaphthalene is not observed with the KX zeolite catalyst. 2,6-diiodonaphthalene is a kinetic product. High conversions and diffusion effects increase the residence time of 2,6-diiodonaphthalene in the zeolite, and the ultimate selectivity to 2,6-diiodonaphthalene is reduced through further oxyiodination reactions and disproportionation reactions. Through proper catalyst design and control of the reaction conditions, excellent yields of 2-iodonaphthalene and 2,6-diiodonaphthalene can be achieved.

REFERENCES

1. De La Mare, P. B. D., and Ridd, J. H., "Aromatic Substitution Nitration and Halogenation, p. 110. Butterworths, London, 1959.
2. (a) Merkushev, E. B., *Synthesis*, 923 (1988); (b) Merkushev, E. B. *Russ. Chem. Rev. (Engl. Transl.)* **53,** 343 (1984).
3. Derbyshire, D. H., and Waters, W. A., *J. Chem. Soc.*, 3694 (1950).
4. Radner, F., *J. Org. Chem.* **53,** 3548 (1988).
5. (a) Paparatto, G., and Saetti, M., Eur. Pat. Appl. EP 181790, 1986; (b) Paparatto, G., and Saetti, M., Eur. Pat. Appl. EP 183579, 1986.
6. (a) Rule, M., Tustin, G. C., Lane, D. W., and Larkins, T. H., U.S. Patent US 4778940, 1988; (b) Rule, M., Tustin, G. C., Lane, D. W., and Larkins, T. H., U.S. Patent US 4746758, 1988; (c) Rule, M., Tustin, G. C., Lane, D. W., and Larkins, T. H. U.S. Patent US 4778938, 1988.
7. Rule, M., Tustin, G. C., Lane, D. W., and Larkins, T. H., U.S. Patent US 4792641, 1988.
8. (a) Rule, M., Fagerburg, D. R., Watkins, J. J., and Fauver, J. S., U.S. Patent US 4786713, 1988; (b) Rule, M., U.S. Patent US 4792634, 1988; (c) Rule, M., Fagerburg, D. R., Watkins, J. J., and Fauver, J. S., U.S. Patent US 4855393, 1989.
9. Rule, M., Larkins, T. H., Lane, D. W., and Steinmetz, G. R., U.S. Patent US 4866200, 1989.
10. Tustin, G. C., Smith, K. C., and Rule, M., U.S. Patent US 4853480, 1989.
11. Kuhl, G. H., *Zeolites* **7,** 251 (1987).
12. Charnell, J. F., *J. Cryst. Growth* **8,** 291 (1971).
13. Hathaway, P. E., and Davis, M. E., *J. Catal.* **116,** 263 (1989).
14. Breck, D. W., "Zeolite Molecular Sieves: Structure, Chemistry and Use," p. 176. Wiley, New York, 1974.
15. Palekar, M. G., and Rajadhyaksha, R. A., *Catal. Rev.—Sci. Eng.* **28,** 371 (1986).
16. (a) Weisz, P. B., and Prater, C. D., *in* "Advances in Catalysis." W. G. Frankenburg, V. I. Komarewsky, and E. K. Rideal, Eds., Vol. VI, p. 143. Academic Press, New York, 1954; (b) Haag, W. O., Lago, R. M., and Weisz, P. B., *Faraday Disc. Chem. Soc.* **72,** 317 (1982)
17. Satterfield, C. N., "Mass Transfer in Heterogeneous Catalysis," p. 4. Krieger, Malabar, Florida, 1981.
18. (a) Barrer, R. M., and Wasilewski, S., *Trans. Faraday Soc.* **57,** 1140 (1961); (b) Barrer, R. M., and Wasilewski, S., *Trans. Faraday Soc.* **57,** 1153 (1961).
19. (a) Breck, D. W. "Zeolite Molecular Sieves: Structure, Chemistry and Use," p. 645. Wiley, New York, 1974; (b) Chen, N.Y., *J. Phys. Chem.* **80,** 60 (1976); (c) Olson, D. H., Haag, W. O., and Lago, R. M., *J. Catal.* **61,** 390 (1980); (d) Nakamoto, H., and Takahashi, H., *Zeolites* **2,** 67 (1982).
20. Laidler, K. J., "Chemical Kinetics," 3rd ed., p. 241. Harper Collins: New York, 1987.
21. Satterfield, C. N., "Mass Transfer in Heterogeneous Catalysis," p. 138. Krieger, Malabar, Florida, 1981.
22. Hougen, O. A., and Watson, K. M., *Ind. Eng. Chem.* **35,** 529 (1943).
23. Pagni, R. M., Kabalka, G. E., Boothe, R., Gaetano, K., Stewart, L. J., Conaway, R., Dial, C., Gray, D., Larson, S., and Luidhardt, T., *J. Org. Chem.* **53,** 4477 (1988).
24. Galli, C., *J. Org. Chem.* **56,** 3238 (1991).
25. (a) Ramamurthy, V., Casper, J. V., Eaton, D. F., Kuo, E. W., and Corbin, D. R. *J. Am. Chem. Soc.* **114,** 3882 (1992); (b) Ramamurthy, V., Casper, J. V., Corbin, D. R., Schlyer, B. D., and Maki, A. H., *J. Phys. Chem.* **94,** 3391 (1990); (c) Ramamurthy, V., Corbin, D. R., and Eaton, D. F., *J. Org. Chem.* **55,** 5269 (1990); (d) Ramamurthy, V., Eaton, D. F., and Casper, J. V., *Acc. Chem. Res.* **25,** 299 (1992); (e) Al-Zaid, K., Owaysi, F., Akashah, S., and Eltekov, Y. A., *in* "Zeolites: Facts, Figures, Future," (P. A. Jacobs and R. A. van Santen, Eds.) p. 945. Elsevier, Amsterdam, 1989.

26. (a) Renouprez, A. J., Jobic, H., and Oberthur, R. C., *Zeolites* **5,** 222 (1985); (b) Fitch, A. N., Jobic, H., and Renouprez, A., *J. Chem. Soc., Chem. Commun.,* 284 (1985); (c) Fitch, A. N., Jobic, H., Renouprez, A., *J. Phys. Chem.* **90,** 1311 (1986); (d) Hepp, M. A., Ramamurthy, V., Corbin, D. R., and Dybowski, C., *J. Phys. Chem.* **96,** 2629 (1992).
27. (a) Barthomeuf, D., *in* "Catalysis and Adsorption in Zeolites" (G. Ohlmann, H. Pfeifer, and R. Fricke, Eds.), p. 157. Elsevier, Amsterdam, 1991; (b) Barthomeuf, D., de Mallmann, A., *in* "Innovation in Zeolite Materials Science" (P. J. Gorbet, W. J. Mortier, E. F. Vansant, and G. Schulz-Ekloff, Eds.), p. 365. Elsevier, Amsterdam, 1988.
28. (a) Ozin, G. A., Ozkar, S., and Stucky, G. D., *J. Phys. Chem.* **94,** 7562 (1990); (b) Ozin, G. A., Ozkar, S., and McMurray, L., *J. Phys. Chem.* **94,** 8289 (1990).
29. Gavriliv, A. P., Kochubei, V. F., and Moin, F. B., *Kinet. Catal. (Engl. Transl.)* **17,** 978 (1976).
30. For a general treatment of this type of kinetic sequence: Pannetier, G., and Souchay, P., "Chemical Kinetics" pp. 196, 204. Elsevier, Amsterdam, 1967.
31. (a) March, J., "Advanced Organic Chemistry: Reactions, Mechanisms,and Structure" pp. 241, 384. McGraw–Hill, New York, 1968; (b) Hine, J., "Physical Organic Chemistry" p. 87. McGraw–Hill, New York, 1962.